Energy Proceedings
Vol 38, 2024
ISSN 2004-2965

Reduced-graphene-oxide-modified nickel foam as anode electrode for increased performance of a non-aqueous thermally regenerative flow battery

Yichao An[1,2], Fang Zhou[1,2], Yu Shi[1,2], Liang Zhang[1,2*], Jun Li[1,2], Qian Fu[1,2], Xun Zhu[1,2], Qiang Liao[1,2]

1 Key Laboratory of Low-grade Energy Utilization Technologies and Systems, Chongqing University, Ministry of Education, Chongqing, 400030, China

2 Institute of Engineering Thermophysics, School of Energy and Power Engineering, Chongqing University, Chongqing, 400030, China
(*Corresponding Author: liangzhang@cqu.edu.cn)

ABSTRACT

Non-aqueous thermally regenerative flow battery (TRFB) has shown great promise to convert low-grade waste heat into electricity for its high circuit voltage and high power density. Developing a reasonable porous anode electrode is essential for the fluid-solid interaction of the anolyte. In this study, a reduced-graphene-oxide-modified nickel foam (RGO/NF_T) was developed to optimize the anode electrode structure and hopefully obtain a competitive performance of TRFB. It was demonstrated that the RGO/NF_T as the anode electrode with better wettability and a larger specific area was beneficial for the electricity generation of TRFB. TRFB using relatively low-cost untreated nickel foam as anode (TRFB-NF) obtained a maximum power density of 105.7 W/m^2, which was similar with that of TRFBs using RVC anode. A further 21% increase in the maximum power density was found in TRFB-RGO/NF_T (127.9 W/m^2). Moreover, the discharging time was extended by 78% and the energy density was improved by 165% in TRFB-RGO/NF_T, in comparison with the TRFB-NF. The results indicated that RGO/NF_T could be a potential anode electrode for TRFBs having the competitive performance in future practical application.

Keywords: thermally regenerative flow battery, non-aqueous, reduced graphene oxide, maximal power generation.

NONMENCLATURE

Abbreviations	
TRFB	The non-aqueous thermally flow regenerative battery
RVC	Reticulated glass carbon
NF	Nickel foam
NF_T	Pretreated nickel foam
RGO/NF_T	The nickel foam loaded with reduced graphene oxide
Symbols	
I	Current
U	Voltage
P_s	Power density
E	Energy efficiency
Q	Electricity capacity
η_Q	Columbic efficiency
η_E	Energy efficiency

1. INTRODUCTION

A large amount of the low-grade heat energy (130 ℃) generated in industrial production and geothermal and solar-based systems has drawn increasing attention due to its potential for carbon-neutral electricity generation [1, 2]. According to the statistics, 20%-50% of total energy consumption in industries was wasted as low-grade waste heat [3, 4]. The emission of low-grade waste heat would lead to a tremendous part of energy loss and heat pollution [5]. Harvesting low-grade waste heat is essential to improve the energy utilization ratio and prohibit emission [6, 7]. However, due to the low difference in temperature and the unconcentrated distribution, heat recovery technologies still struggle with poor performance. Among the various approaches for harvesting heat, thermo-electric conversion systems based on electrochemical reactions have been one of the most promising and widely investigated. Related technologies mainly include the thermo-electrochemical cell (TEC) [8, 9], thermally regenerative electrochemical cycle (TREC) [10], thermally regenerative battery (TRB)

This is a paper for 15th International Conference on Applied Energy (ICAE2023), Dec. 3-7, 2023, Doha, Qatar.

[11], and direct thermal charge cell (DTCC) [12]. Thereinto, TRB has high open circuit voltage and power density, simple operation, and mild reaction conditions, showing great potential for development.

In 2015, the thermally regenerative battery based on the reaction of copper and ammonia was first proposed to harvest low-grade waste heat, exhibiting a relatively higher electricity generation [11]. It could be divided into two parts, electric generation, and thermal regeneration.

Low-grade waste heat was applied to regenerate the active substance, and the concentration difference of it between anolyte and catholyte led to the chemical potential. In that way, the multiple batches of electricity production were realized using low-grade waste heat. To improve the maximum power density and stability, new reactors, composite porous electrodes, and different reaction systems were studied in subsequent papers [13-15]. To enhance mass transfer in the batteries, a flow TRB [16] and a fluidized-bed reactor [17] were developed, which improved the electricity generation performance of TRB. In addition, the original reaction was substituted for the increase in electricity generation of TRBs, such as copper-ethylenediamine, silver-ammonia [18], and copper/zinc-ammonia [19]. That led to important increases in TRBs. Considering the corrosion of anode electrodes in traditional TRB led to the decrease in service life and cycling stability, the composite porous electrode built on a stable skeleton could be the most possible solution [20, 21]. Although much research has been carried out to enhance the electric generation of TRBs, the low solubility of reactants still limits the open circuit voltage of TRBs. Meanwhile, the small difference in the boiling temperature of water and decomplexation temperature in traditional TRB would lead to the vaporization of water would consume more heat energy. To solve these problems, a non-aqueous thermally regenerative flow battery (TRFB) was proposed [22]. The solubility of reactants was improved essentially for the organic solvent. And the larger difference between the boiling temperature and decomplexation was expected to improve the utilization of heat energy. The working principle is shown in Figure 1a, and the anode and cathode reaction equations are as follows:

Cathodic reaction:

$$Cu^{2+} + e^{-} \rightarrow Cu^{+}$$

Anodic reaction:

$$Cu(s) - e^{-} \rightarrow Cu^{+}$$

Thermal regeneration：

$$2Cu(CH_3CN)_4^{+} \xrightarrow{\Delta} Cu(s) + Cu^{2+} + 8CH_3CN$$

It is worth noting that the TRFB was not only regenerated by low-grade waste heat but also a direct charging battery storing electric energy, which lead to a wider potential application. However, less research on TRFB was performed, especially the liquid-solid flow of anolyte. The porous anode electrode was essential to the liquid-solid flow and the electrochemical reactions in TRFB [23]. The anode electrode was currently the reticulated glass carbon, which has a smaller specific area, lower wettability, and higher economic cost, limiting the enhancement and application of TRFB.

Considering that the good conductivity and wettability of the low-cost nickel foam, it is expected to improve the electric production performance of the battery as a skeleton. Thus, the nickel foam with a dilute hydrochloric acid treatment and reduced graphene oxide (RGO) modification was proposed to improve the wettability and promote the specific area of the anode electrode. The physicochemical properties of different anode electrodes (RVC, untreated nickel foam, treated nickel foam, RGO-modified treated nickel foam) were characterized and compared, and their effects on the performance of TRFB were investigated.

2. MATERIAL AND METHODS

2.1 The preparation of the electrode

The nickel foam loaded with reduced graphene oxide (RGO/NF_T) was prepared by one spot reduction, as shown in Fig 1b. The impurities of untreated nickel foam (NF) were washed away by the acetone (Chengdu Colon Chemicals Co. LTD) and the alcohol (Shanghai Titan Technology Co., LTD). And the metallic oxide on the surface was erased by the dilute hydrochloric acid (Chengdu Colon Chemicals Co. LTD, 1.2 mol L^{-1}). Then the pretreated nickel foam (NF_T) was obtained after several washings and a vacuum drying of 3 h at 60 ℃. NF_T was dipped into graphene oxide dispersion (Aladdin, 1mg mL^{-1}, 10mL) for 20 min, and dried naturally. The process was repeated for 5 times to ensure the successful deposition of graphene oxide. Then the electrodes were immersed in the ascorbic acid (Chengdu Colon Chemicals Co. LTD, 20mL, 10 mg/mL) to produce reduced graphene oxide at 60 ℃ for 6 h. The obtained electrodes were washed several times with deionized water. And the RGO/NF_T was obtained after freeze-drying for 12 h.

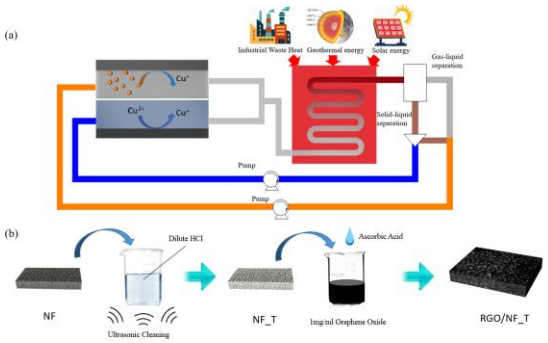

Fig. 1. The working principle of non-aqueous thermally regenerative flow battery (a); The construction process of the nickel foam loaded with reduced graphene oxide (b).

2.2 The construction and operation of TRFB

The compact reactor of TRFB consists of two waist circular chambers (20×10×2 mm) and a cation exchange membrane (Fumasep, FAB-PK-130), which is used to divide the anode chamber and cathode chamber. The TRFB reactor is secured by bolts through the guide plate (80 x 50 x 2 mm) and the end plate, with a gasket in the middle to prevent electrolyte leakage. The generated electrons were recorded by an electrochemical workstation through the end plate. In addition, the reaction chamber and the baffle are titanium plating gold to reduce the transmission impedance of electrons. The solvents of anode and cathode electrolyte are acetonitrile (ACN) and propylene carbonate (PC) (Shanghai Titan Technology Co., LTD) with a volume ratio of 1:1. Tetraethylamine tetrafluoroborate (TEABF4, Shanghai Titan Technology Co., LTD, 0.15 mol/L) is the supporting electrolyte in the anolyte and the catholyte. The nano copper slurry (Qinghe County Xindun Metal Material Co. LTD, 500 nm) is blended with anolyte to form a stable nanofluid with magnetic agitation. Cu^{2+} in the cathode solution is obtained by charging tetrafluoroborate tetraethylcyanide copper (I) (Shanghai Haohong Biomedical Technology Co., LTD., 0.1 mol /L) at a constant current of 35 mA. To avoid the oxidation of nano copper and Cu^{+} by air, the assembly and operation of TRFB should be carried out in an oxygen-free operating box. The volume of anode and cathode electrolyte of a single battery is 20 mL. And the flows from the electrolyte tank into the reactor chamber at a fixed flow rate (35 mL/min) were realized through the peristaltic Pump (Longer pump BT100-1J).

2.3 Material and Methods

Scanning electron microscopy (3400 N, HITACHI instrument) and Energy Dispersive Spectroscopy (EDS, Apollo XLT SDD, EDAX) were used to observe and analyze the microscopic morphology of the electrodes, which provided visual pore distribution on the electrode surface. The physical adsorption method (BET, ASAP 2460) was used to analyze the distribution of the pore size and the specific surface area of the electrode. The polarization experiments of the battery were performed by linear sweep voltammetry (LSV) with an electrochemical workstation (Princeton). The scanning voltage range was set according to the open circuit voltage of the battery, and the scanning rate was 1 mV/s.

2.4 Section of theory/calculation

The output power density of the battery was $P_s = UI/S$, where *S* was the projected electrode area of the three-dimensional porous electrode, 1×10^{-4} m^2. The current density was calculated as $I_s = I/S$. The discharging current of the battery was 15 mA, and the actual energy density of TRFB was calculated by $E = \int UIdt/V$, where *V* was the volume of the electrolytes (*V*=20 mL). The discharge capacity of TRFB was calculated as $Q = It$ where *t* stands for the discharging time. In a non-aqueous thermal regenerative flow battery, the coulombic efficiency η_Q of the battery was calculated as $\eta_Q = \frac{QM}{nmVF}$, where *Q* was the discharge capacity, *n* was the number of reaction electrons, *m* and *M* was the mass and molecular weight of the reactant respectively, *F* was the Faraday constant, *F* = 96485 C/mol. The energy efficiency η_E was set as the ratio of the actual energy density to theoretical energy density during discharging, calculated as $\eta_E = \frac{E}{\Delta G} = \frac{\int UIdt_h/V}{ncFE_0}$.

3. RESULTS AND DISCUSSION

3.1 The comparison of different electrodes

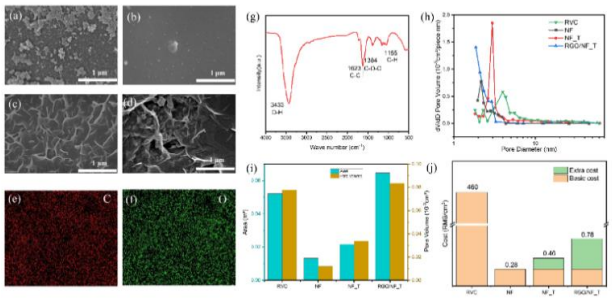

Fig. 2. The SEM images of RVC (a), NF (b), NF_T (c), RGO/NF_T (d) and the EDS mapping of RGO/NF_T (C element (e), O element (f)); The FT-IR images of RGO/NF_T(g); The pore distribution (h), the specific surface area (i) and the economic cost (j) of different electrodes.

To compare and analyze the microstructure of different electrodes visually, the scanning electron

microscope (SEM) and energy dispersive spectrometer were applied and the results were shown in Figure 2(a-d). The rough interface of RVC caused by the stacking particles showed a potentially high specific surface area. And the smooth skeleton of NF was etched to be a rough wrinkle structure by dilute hydrochloric acid for the elimination of metallic oxide on the surface. That could lead to an increase in the specific surface area of NF. After the RGO was loaded on the surface, the resulting porous morphology of RGO/NF_T would possibly lead to an increase in specific surface area and electrochemically active site. The electrochemical reaction surface and the reaction rate would be affected directly by the morphology of the electrodes. Moreover, the EDS and FT-IR tests were carried out to exhibit the uniform distribution of the C element and O element, as shown in Figure 2(e, f). The C and O were distributed uniformly on the nickel foam. And the rich functional groups were exhibited, such as the -OH group (characteristic peak 3433), and C-O-C (characteristic peak 1384), which was consistent with the results of RGO [24]. That demonstrated the even distribution of RGO on the nickel foam. The physical adsorption tests were performed to analyze the pore distribution of the electrodes, as shown in Figure 2(h, i). Considering that the density of RVC was far higher than the nickel foam, thus the specific surface area was converted to surface area based on the same size (10*10*3 mm). Thereinto, the surface area of NF was the smallest (0.013 m^2). The surface area of RGO/NF_T was 5 times of NF, which was 0.065 m^2. The increase in surface area was mainly due to the aggregability of graphene oxide, forming a lot of microporous structures during the reduction process (pore size <2 nm). Although the surface area of RVC was relatively larger than NF and NF_T, the actual electrochemical reaction area was still unknown for the wettability of the electrodes. Better wettability meant a larger electrochemical effective reaction area, which would contribute to the increase of electric generation of TRFB. Moreover, the economic cost of NF was far lower than RVC (1/1642), and the cost of RGO/NF_T was almost double of NF. If the nickel foam shows better wettability than RVC, that would not only lead to a decrease in the cost of TRFB but also an increase in the electric generation of TRFB.

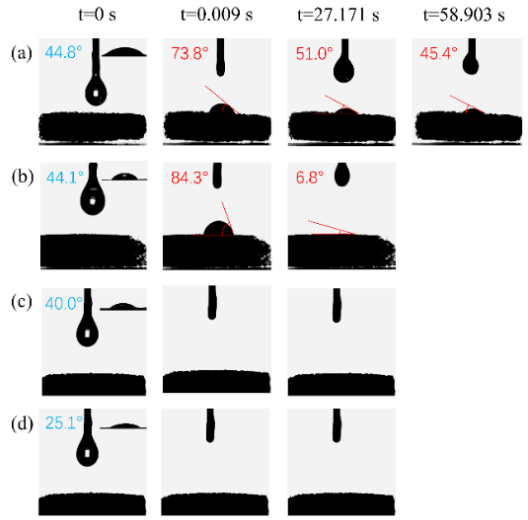

Fig. 3. The intrinsic contact angle (red) and contact angle (blue) at different times of RVC (a), NF (b), NF_T (c), RGO/NF T (d).

As a key factor influencing electrochemical reaction rate, the increase in wettability of electrodes would decrease the transfer resistance of ions and increase the potential effective reaction area [25]. To explore the wettability of different electrodes, the intrinsic contact angle and contact angle of different electrodes were tested, as shown in Figure 3. The wettability of electrodes was mainly influenced by the intrinsic contact angle and pore structure. To reveal the wettability of the electrodes on the organic electrolytes, the anolyte without nano copper was chosen as the test solution. The intrinsic contact angle of RVC (44.8°) was similar to NF (44.8°). Due to the erosion caused by the dilute hydrochloric acid [26], the intrinsic contact angle of NF_T was decreased to 40°. Moreover, the intrinsic contact angle of RGO/NF_T was decreased to 25.6° for the polar functional groups of RGO [27]. That could cause the decrease of transfer resistance of active substances, enhancing the electricity generation of TRFB. And the penetration time of different electrodes was analyzed to verify the good wettability of electrodes on non-nanoparticle anolyte. After 27.2 s, the contact angle of RVC decreased by 31%, and the NF decreased by 90%, showing that the wettability of NF was better than RVC. At this time, the drop had immersed into the nickel foam, while the RVC need extra 152.8 s. That might be due to the disadvantageous structure of RVC, which increased the transfer resistance of electrolytes. It might even lead to complete noninfiltrating regions of the electrodes and a reduction of the effective reaction area, limiting the electric generation of TRFB.

In conclusion, the low cost and better wettability of NF make it more competitive than RVC, regardless of the

smaller surface area. Based on that, the wettability and surface area were enhanced by loading RGO on NF, which would decrease the transfer resistance and increase the number of active sites. That might be able to further improve the electricity generation of TRFB.

3.2 Maximal power generation of TRFBs using different anode electrodes

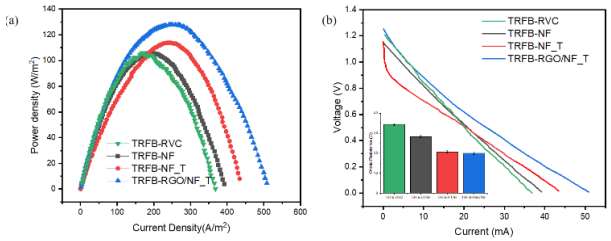

Fig. 4. The power density curve (a), polarization curve (b) of TRFBs using different anode electrodes.

The maximal power generation of TRFBs using different anode electrodes were studied to explore the effect of the anode electrodes, as shown in Figure 4. The open circuit voltage (OCV) was about 1.2 V, which was influenced by the concentration of the reactants. The maximum power density of TRFB-NF (105.7 W/m^2) was close to the TRFB-RVC (106 W/m^2). Although the surface area of RVC was about 3 times of NF, the worse wettability of RVC shortened the effective reaction area and limited the electricity generation. Meanwhile, after fitting the polarization curve, the ohmic resistance of TRFB-RVC (38.3 Ω) was 1.2 times of TRFB-NF (28.3 Ω). That meant that the larger loss of electron transfer was also the reason for the limitation of TRFB-RVC. Poor wettability and conductivity of RVC greatly limit the optimization of TRFB. The composite electrode built on the NF would possibly strengthen the electricity generation of TRFB. The maximum power density of TRFB-NF_T was increased to 113.9 W/m^2 for the increased surface area (65%) and the decreased ohmic resistance (27%). Furthermore, the maximum power density of TRFB-RGO/NF_T (127.9 W/m^2) was increased by 21%, compared to the TRFB-NF. That was mainly due to the increase in surface area and the improvement of the wettability of electrodes. In addition, the ohmic resistance of TRFB-RGO/NF_T (19.9 Ω) was decreased a bit for the little electron resistance of RGO.

3.3 Electricity generation of TRFBs using different anode electrodes

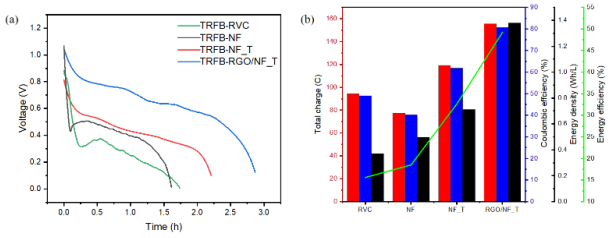

Fig. 5. The discharge curve (a), and the efficiencies (b) of TRFBs using different anode electrodes.

What's more, the electricity generation of the TRFBs of different anode electrodes were studied at a constant current (15 mA/cm^2), as shown in Figure 5a. The voltage of all the TRFBs decreased rapidly at first to a relatively stable discharging platform, caused by the decrease of the concentration of reactants. Thereinto, the voltage platform of TRFB-RGO/NF_T was the highest (635.9 mV) for 2.9 h. That led to an increase in electricity generation (155.6 C) and energy density (1.38 Wh/L) relative to TRFB-NF. Meanwhile, the energy density of TRFB-RGO/NF_T was increased by 165%, compared to TRFB-NF. The superiority of the RGO/NF_T anode electrode was proved by its good electricity generation. The abundant pore structure of RGO/NF_T contributed to the rapid electrochemical reaction kinetics. And the excellent wettability of RGO/NF_T enhanced the mass transfer at the electrode interface, which effectively weakened the ohmic polarization phenomenon. In conclusion, the RGO/NF_T could be a competitive potential electrode for the practical application of TRFB.

4. CONCLUSIONS

To enhance the electricity generation of non-aqueous thermally regenerative flow batteries (TRFBs), the nickel foam loaded with reduced graphene oxide (RGO/NF_T) was proposed as the anode electrode. The low cost and good wettability make the NF more competitive than the RVC, with almost the same maximum power density. Moreover, the electricity generation of TRFB-NF_T was enhanced for the increase of surface area, which was developed by the dilute hydrochloric acid. And the electricity generation was further optimized with RGO/NF_T anode electrode, caused by an increase in surface area and the improvement of the wettability. The maximum power density of the TRFB-RGO/NF_T (127.9 W/m^2) was increased by 21% and the energy density (1.38Wh/L) was increased by 165%, compared to the TRFB-NF.

ACKNOWLEDGEMENT

This work was supported by the National Natural Science Foundation of China (No. 51976018), Innovative

Research Group Project of the National Natural Science Foundation of China (No. 52021004), Natural Science Foundation of Chongqing, China (CSTB2022NSCQ-MSX1596), and Scientific Research Foundation for Returned Overseas Chinese Scholars of Chongqing, China (No. cx2021088)

DECLARATION OF INTEREST STATEMENT

The authors declare that they have no known competing financial interests or personal relationships that could have appeared to influence the work reported in this paper. All authors read and approved the final manuscript.

REFERENCE

[1] Chu S, Majumdar A. Opportunities and challenges for a sustainable energy future. Nature 2012;488:294-303.

[2] Lu H, Price L, Zhang Q. Capturing the invisible resource: Analysis of waste heat potential in Chinese industry. Appl Energ 2016;161:497-511.

[3] Qyyum MA, Khan A, Ali S, Khurram MS, Mao N, Naquash A, et al. Assessment of working fluids, thermal resources and cooling utilities for Organic Rankine Cycles: State-of-the-art comparison, challenges, commercial status, and future prospects. Energ Convers Manage 2022;252:115055.

[4] Yuan ZW, Wei L, Afroze JD, Goh K, Chen YM, Yu YX, et al. Pressure-retarded membrane distillation for low-grade heat recovery: The critical roles of pressure-induced membrane deformation. J Membrane Sci 2019;579:90-101.

[5] Wang DX, Ling X, Peng H, Liu L, Tao LL. Efficiency and optimal performance evaluation of organic Rankine cycle for low grade waste heat power generation. Energy 2013;50:343-52.

[6] Forman C, Muritala IK, Pardemann R, Meyer B. Estimating the global waste heat potential. Renew Sust Energ Rev 2016;57:1568-79.

[7] Shi Y, Zhang L, Li J, Fu Q, Zhu X, Liao Q, et al. Effect of operating parameters on the performance of thermally regenerative ammonia-based battery for low-temperature waste heat recovery. Chinese J Chem Eng 2021;32:335-40.

[8] Pourkiaei SM, Ahmadi MH, Sadeghzadeh M, Moosavi S, Pourfayaz F, Chen L, et al. Thermoelectric cooler and thermoelectric generator devices: A review of present and potential applications, modeling and materials. Energy 2019;186:115849.

[9] Battistel A, Peljo P. Recent trends in thermoelectrochemical cells and thermally regenerative batteries. Curr Opin Electroche 2021;30:100853.

[10] Zhang H, Lek DG, Huang S, Lee YM, Wang Q. Efficient Low-Grade Heat Conversion and Storage with an Activity-Regulated Redox Flow Cell via a Thermally Regenerative Electrochemical Cycle. Adv Mater 2022;34:2202266.

[11] Zhang F, Liu J, Yang WL, Logan BE. A thermally regenerative ammonia-based battery for efficient harvesting of low-grade thermal energy as electrical power. Energ Environ Sci 2015;8:343-9.

[12] Wang X, Huang Y, Liu C, Mu K, Li KH, Wang S, et al. Direct thermal charging cell for converting low-grade heat to electricity. Nat Commun 2019;10:4151.

[13] Zhang YS, Zhang L, Li J, Zhu X, Fu Q, Liao Q, et al. Performance of a thermally regenerative ammonia-based flow battery with 3D porous electrodes: Effect of reactor and electrode design. Electrochim Acta. 2020;331.

[14] Zhang L, Li YX, Zhu X, Li J, Fu Q, Liao Q, et al. Copper Foam Electrodes for Increased Power Generation in Thermally Regenerative Ammonia-Based Batteries for Low-Grade Waste Heat Recovery. Ind Eng Chem Res 2019;58:7408-15.

[15] Chen PY, Shi Y, Zhang L, Li J, Zhu X, Fu Q, et al. Performance of a Thermally Regenerative Battery with 3D-Printed Cu/C Composite Electrodes: Effect of Electrode Pore Size. Ind Eng Chem Res. 2020;59:21286-93.

[16] Shi Y, Zhang L, Li J, Fu Q, Zhu X, Liao Q, et al. 3-D printed gradient porous composite electrodes improve anodic current distribution and performance in thermally regenerative flow battery for low-grade waste heat recovery. J Power Sources 2020;473.

[17] Zhang YS, Shi Y, Zhang L, Li J, Fu Q, Zhu X, et al. A fluidized-bed reactor for enhanced mass transfer and increased performance in thermally regenerative batteries for low-grade waste heat recovery. J Power Sources 2021;495.

[18] Rahimi M, Kim T, Gorski CA, Logan BE. A thermally regenerative ammonia battery with carbon-silver electrodes for converting low-grade waste heat to electricity. J Power Sources 2018;373:95-102.

[19] Wang WG, Shu GQ, Tian H, Huo DX, Zhu XP. A bimetallic thermally-regenerative ammonia-based flow battery for low-grade waste heat recovery. J Power Sources 2019;424:184-92.

[20] Chen PY, Zhang L, Shi Y, Li J, Fu Q, Zhu X, et al. Biomass waste-derived hierarchical porous composite electrodes for high-performance thermally regenerative ammonia-based batteries. J Power Sources 2022;517.

[21] Shi Y, Zhang L, Zhang YS, Li J, Fu Q, Zhu X, et al. Construction of a hierarchical porous surface composite

electrode by dynamic hydrogen bubble template electrodeposition for ultrahigh-performance thermally regenerative ammonia-based batteries. Chem Eng J. 2021;423.
[22] Maye S, Girault HH, Peljo P. Thermally regenerative copper nanoslurry flow batteries for heat-to-power conversion with low-grade thermal energy. Energ Environ Sci 2020;13:2191-9.
[23] Percin K, Rommerskirchen A, Sengpiel R, Gendel Y, Wessling M. 3D-printed conductive static mixers enable all-vanadium redox flow battery using slurry electrodes. J Power Sources 2018;379:228-33.
[24] Wei DQ, Liu X, Lv SH, Liu LP, Wu L, Li ZX, et al. Fabrication, Structure, Performance, and Application of Graphene-Based Composite Aerogel. Materials 2022;15.
[25] Borja-Maldonado F, López Zavala MÁ. Assessment of Graphite, Graphene, and Hydrophilic-Treated Graphene Electrodes to Improve Power Generation and Wastewater Treatment in Microbial Fuel Cells. Bioengineering 2023;10(3):378.
[26] Wang J, Zhang Y, Yu L, Cui K, Fu T, Mao H. Effective separation and recovery of valuable metals from waste Ni-based batteries: A comprehensive review. Chem Eng J 2022;439:135767.
[27] Stobinski L, Lesiak B, Malolepszy A, Mazurkiewicz M, Mierzwa B, Zemek J, et al. Graphene oxide and reduced graphene oxide studied by the XRD, TEM and electron spectroscopy methods. J Electron Spectrosc 2014;195:145-54.